Influence of Stratification and Shoreline Erosion on Reservoir Sedimentation Patterns

Şebnem Elçi[1]; Paul A. Work[2]; and Earl J. Hayter[3]

Abstract: Sedimentation in the main pool of a deep (maximum depth: 50 m), 227 km^2 hydropower reservoir was modeled using a three-dimensional numerical model of hydrodynamics and sedimentation for different wind, inflow, and outflow conditions. Short-term velocity measurements made in the reservoir were used to validate some aspects of the hydrodynamic model. The effects of thermal stratification on sedimentation patterns were investigated, since the reservoir is periodically strongly stratified. Stratification alters velocity profiles and thus affects sedimentation in the reservoir. Sedimentation of reservoirs is often modeled considering only the deposition of sediments delivered by tributaries. However, the sediments eroding from the shorelines can contribute significantly to sedimentation if the shorelines of the reservoir erode at sufficiently high rates or if sediment delivery via tributary inflow is small. Thus, shoreline erosion rates for a reservoir were quantified based on measured fetch, parameterized beach profile shape, and measured wind vectors, and the eroded sediments treated as a source within the sedimentation modeling scheme. The methodology for the prediction of shoreline erosion was calibrated and validated using digital aerial photos of the reservoir taken in different years and indicated approximately 1 m/year of shoreline retreat for several locations. This study revealed likely zones of sediment deposition in a thermally stratified reservoir and presented a methodology for integration of shoreline erosion into sedimentation studies that can be used in any reservoir.

DOI: 10.1061/(ASCE)0733-9429(2007)133:3(255)

CE Database subject headings: Sedimentation; Deposition; EFDC; Shoreline erosion; Reservoir; Stratification.

Introduction

Sedimentation in a reservoir can reduce the useful storage [the volume of water between the minimum pool (e.g., outlet invert elevation) and full pool (e.g., spillway crest elevation) levels] and serious erosion problems may arise downstream due to reduced sediment outflow from the reservoir. This paper describes the erosion and deposition of primarily cohesive sediments transported in a periodically thermally stratified reservoir. The fate of sediments, coming from both tributaries and eroding shorelines, was modeled as a function of varying wind and flow conditions within the main pool of the reservoir.

This study was motivated in part by the high concentrations of polychlorinated biphenyls (PCBs) found in Twelve-Mile Creek, a major tributary of Hartwell Lake, a U.S. Army Corps of Engineers (USACE) reservoir located on the Savannah River, between Anderson, S.C., and Hartwell, Ga. (Fig. 1), resulting from the operation of a capacitor manufacturing facility from 1955 to 1977 (USEPA 1991; Clearwater 1997). Silts and clays often facilitate contaminant transport, since PCBs and other hydrophobic organic chemicals are preferentially adsorbed onto fine-grained sediments. These sediments can be advected over large distances before settling, due to their low settling velocities, particularly in freshwater environments. The main pool of the reservoir was selected as the study domain, in order to model likely depositional zones. Knowledge of these depositional zones is potentially useful for assessment of mitigation options for pollution problems as well as predictions of reservoir lifetime and development of maintenance schemes.

Reservoir sedimentation has been widely studied in the past, often focusing on the description and investigation of the mechanism by which the sediments are transported into the reservoir (Blumberg and Mellor 1987; Blumberg et al. 1999; Falconer et al. 1991; Jin et al. 2000; Rueda and Schladow 2003; Yang et al. 2000). Deposition rates were of primary interest in many cases, for definition of optimal reservoir operation scheme and reservoir lifetime, and were modeled numerically or measured via surveying. However, the contribution of sediments eroding from the shorelines is often overlooked when quantifying sediment deposition in reservoirs. Depending on the erosion rates and sediment delivery by tributaries, eroding sediments can contribute significantly to the total deposition. In Hartwell Lake, for instance, the existence of over 1,500 erosion control structures along the lake's shoreline (as of 2002; USACE Hartwell Lake Office) serves as an indication of the magnitude of the erosion problem. For a more accurate assessment of sedimentation in the reservoir, sediments eroded from the shorelines must be quantified and accounted for in the model as an additional sediment source.

Different methods have been developed to quantify shoreline erosion in lakes and reservoirs. One approach is to predict wave

[1]Assistant Professor Izmir Institute of Technology, Dept. of Civil Engineering, Gülbahçe Campus, 35437 Urla, Izmir, Turkey. E-mail: sebnemelci@iyte.edu.tr

[2]Associate Professor, Georgia Institute of Technology, School of Civil and Environmental Engineering, Savannah Campus, 210 Technology Circle, Savannah, GA 31407-3039. E-mail: paul.work@gtsav.gatech.edu

[3]Research Environmental Engineer, U.S. Environmental Protection Agency, National Exposure Research Laboratory, Athens, GA 30605. E-mail: hayter.earl@epamail.epa.gov

Note. Discussion open until August 1, 2007. Separate discussions must be submitted for individual papers. To extend the closing date by one month, a written request must be filed with the ASCE Managing Editor. The manuscript for this paper was submitted for review and possible publication on July 28, 2005; approved on June 8, 2006. This paper is part of the ***Journal of Hydraulic Engineering***, Vol. 133, No. 3, March 1, 2007. ©ASCE, ISSN 0733-9429/2007/3-255–266/$25.00.

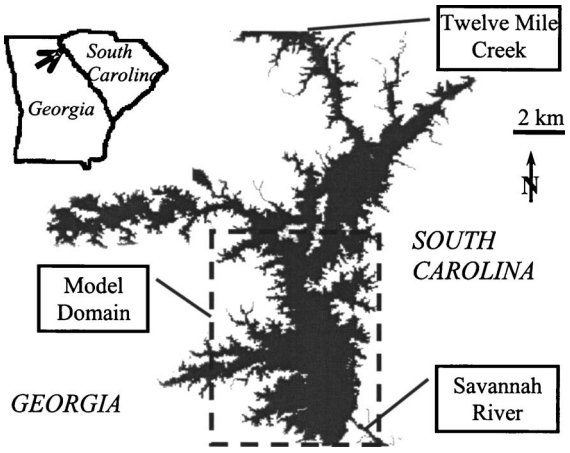

Fig. 1. Map of study site: dashed box shows the region within the main pool of the lake that was modeled to describe circulation, erosion, and sediment deposition patterns

conditions at a given site from available wind time series data. Predicted deep water waves are transformed to nearshore conditions using a numerical or analytical wave transformation model (e.g., Kamphuis and Readshaw 1979). Erosion rate is then empirically related to wave energy or power at breaking (Kamphuis et al. 1986; Nairn et al. 1986; Penner 1993). This approach has some dependence on soil characteristics via an empirical coefficient, but does not account for the geometry of the shoreline profile, among other characteristics. In this study, for assessment of erosion, a method that predicts erosion rate as a function of the shape of the beach profile and wind forcing was developed and applied to Hartwell Lake. Based on this analysis, eroded sediments were quantified and treated as a sediment source to investigate their fate and impact on the overall sediment budget.

The complexities of the hydrodynamic processes in a reservoir suggest the use of numerical modeling approaches to provide a description of circulation, mixing, and density stratification. Hydrodynamic models use reservoir geometry, inflows, withdrawals, and meteorological data to simulate water levels, flow velocities, and temperatures. In a reservoir, wind-generated surface stresses, buoyancy or density forcing, turbulent momentum, and mass transport should all be simulated by the model.

In this paper, a numerical hydrodynamic model is applied to Hartwell Lake to simulate lake response to wind forcing and inflows and/or outflows, and results are compared to short-term velocity measurements made by the writers. Simulations of longer-term sediment deposition patterns (with input data defined based on statistical analysis of ten years of measured data) for different climate and flow conditions in the reservoir are then presented and discussed. The effect of stratification on deposition patterns is investigated. Following the description of the improved methodology for shoreline erosion quantification, incorporation of this methodology into the sedimentation modeling scheme is presented and results discussed.

Modeling of Hydrodynamics in the Reservoir

As will be demonstrated, flows in the reservoir are strongly three-dimensional; thus a three-dimensional (3D) hydrodynamic model was necessary to simulate reservoir flows and sedimentation. A widely used and tested model with the capability of simulating stratified flows and the transport of cohesive sediments was required. The Environmental Fluid Dynamics Code (EFDC) developed by Hamrick (1996) was selected for this purpose.

EFDC Model

The EFDC model solves the three-dimensional, vertically hydrostatic, free surface, turbulent averaged equations of motion for a variable density fluid. The model uses a stretched (sigma) vertical coordinate and Cartesian or curvilinear, orthogonal horizontal coordinates. Dynamically coupled transport equations for turbulent kinetic energy, turbulent length scale, salinity, and temperature are also solved. An equation of state relates density to pressure, salinity, temperature, and suspended sediment concentration. The numerical scheme employed in EFDC to solve the governing equations uses a second-order accurate spatial finite-difference scheme on a staggered or *C* grid. The model has been applied to several water systems (Ji et al. 2000, 2001; Jin et al. 2000, 2002; Jin and Ji 2001; Kim et al. 1997; Shen et al. 1999; Shen and Kuo 1999; Tetra Tech 1999). For a detailed description of EFDC, the reader is referred to Hamrick (1996).

Hydrodynamic circulation patterns in the main pool of Hartwell Lake are mainly controlled by wind, inflows, outflows, and thermal stratification. Daily inflow and outflow data for Hartwell Lake were obtained from the USACE. Outflows are computed by converting the electrical power measured at the power plant into discharge, and inflow values are derived from a volume balance of the reservoir. Thus, the published inflow values include the net impact of rainfall, surface water runoff, groundwater inflows and outflows, and evapotranspiration. Wind data were obtained from the National Oceanic and Atmospheric Administration for Greenville–Spartanburg Airport, S.C., located 65 km northeast of the lake. Hourly wind speed and direction data were available for the period from 1962 to the present.

The computational mesh for the hydrodynamic and sediment transport model was constructed using digital elevation model data composed of four different 7.5 minute (scale: 1:24,000, projection: UTM, spatial resolution: 30 m) quadrangle maps (South Carolina Department of Natural Resources). The boundaries of the model domain were selected so that the main pool of the reservoir could be represented. The location of the dam determined the downstream boundary, and the confluence of the two main tributaries was taken as the upstream boundary. The computational grid had 51×94 horizontal cells, each 150 m $\times$ 150 m, and 10 vertically stretched layers, each with a fractional thickness of 10% of the water depth. A 60-s time step was used in simulations after testing for numerical stability. Initial water depths were set to match the data obtained from digitized topographic maps and from measured water stage. Initial velocities were set to zero. Water column temperatures were initialized at 10°C (constant in space), in agreement with the conditions during the field measurement period. The model was run for 20 days with the actual climate and flow data prior to the period of field measurements, since initial conditions (i.e., velocities, temperatures) were approximated.

The river inflows and controlled outflow at the dam were simulated as sources and sinks in the model system. At upstream boundaries, the river inflow was uniformly distributed across the inflow cross section. The sediment inflow was assumed proportional to the river inflow as discussed below. The controlled outflow at the dam was specified at one cell (essentially a point sink) at the downstream boundary.

J. Hydraul. Eng., 2007, 133(3): 255-266

Field Measurements

Velocities and depths at selected transects in Hartwell Lake were measured using a 1200 kHz acoustic Doppler current profiler (ADCP) and fathometer deployed from a small boat while underway. Since Hartwell Lake is 50 m deep, the bottom was out of range of the instrument, and only the velocities for the top 10–15 m of the water column could be measured. The navigation information provided by a global positioning system receiver was used to convert the relative velocities reported by the ADCP to the earth's reference frame. Measured data were averaged every 30 s and profiles acquired with a bin size (vertical resolution) of 1 m.

The field data were collected during February 10–14, 2003. Throughout that week, very strong winds (approximately 4 times the historical average of 3 m/s) from the southwest were observed. The temperature profile throughout the water column was constant at about 9 °C. Boat speed was maintained near 2.5 m/s and the measured mean flow speeds within the surface layer were as high as 30 cm/s.

Comparison of Simulated and Measured Velocities

Fig. 2 shows the near-surface velocity vectors measured at two transects after correction for boat velocity. Reported surface velocities represent velocities averaged over the top bin thickness of 1 m below the instrument's blanking distance of 0.44 m.

The measured velocities were filtered to discard measurements for which the error velocities exceeded 5 cm/s (20% of the typical average velocity). Comparison of simulated and measured speeds indicated differences of less than 20% (4–6 cm/s) of the maximum measured values for all transects without any calibration of model parameters. The results improved for the bottom transect shown in Fig. 2 (along which the depth reaches to 40 m), when model surface layer thickness was reduced from 10 to 5% of the water depth to facilitate comparison to the measurements. Errors in speed were reduced to 3 cm/s. Jin et al. (2000) and Rueda et al. (2003) both reported velocity errors up to 5 cm/s when measuring mean flows via similar techniques in lakes with fetches ranging from 15–45 km. In the case discussed here, the simulated values were typically lower than the measured velocities, but still in reasonable agreement even without any parameter calibration.

A review of similar modeling studies revealed that several other numerical models systematically underpredicted measured velocities as well (Jin et al. 2000; Rueda et al. 2003; Blumberg et al. 1999). These comparisons typically indicated an underprediction of velocities in high wind conditions. A possible reason for this finding might be the tendency of some numerical models to simulate more rapid dissipation of energy than occurs in nature. Another possible reason is the underestimation of wind stress exerted on the lake surface. Wind data used in the model simulations were collected at a single station located 65 km from the lake; measurements closer to the site might have yielded slightly different model results.

Deposition of Sediments Coming from Tributaries

Long-term sediment deposition patterns were modeled using the sediment transport module of the EFDC model. A careful examination of available data was necessary to determine which forcing combinations should be simulated to represent long-term deposition patterns, since modeling every single climate condition observed in the past 40 years was not feasible. In order to determine which forcing combinations should be simulated to represent long-term deposition patterns, a statistical analysis of daily mean values of inflow, outflow, and wind data for ten years (1990–1999) was performed. Historical records of wind and flow data were used to determine frequencies of occurrence and representative conditions for prediction of depositional zones.

Sediment size and suspended sediment concentration data were obtained from samples collected by Bechtel at 11 transects of Twelve Mile Creek, a tributary to Hartwell Lake (USEPA 1991). The median grain sizes of the sediment samples varied from 0.0075–0.145 mm. Over half of the sediment samples had more than 50% of the grains in the silt and clay ranges, i.e., grain sizes finer than 0.062 mm. Analysis of the water samples indicated that the total suspended solid concentrations varied from 5.6 mg/L in the furthest downstream station to 46 mg/L in the furthest upstream station, with a mean of 40 mg/L. Based on the values specified above, the cohesive sediment parameters used in the model simulations were selected; these are summarized in Appendix I.

The implications of not using actual sediment loadings to the reservoir would be incorrect quantification of sedimentation rates. The approach described here could be improved upon by applying a sediment rating curve derived from long-term measurements of sediment concentrations, or direct measurements during the period of interest. Bathymetric surveying of the lake revealed that sedimentation in the reservoir was on the order of 5 cm/year in the thalweg. The net sedimentation (up to 2 m) since reservoir construction is not sufficient to significantly alter reservoir circulation patterns. Even if the inaccurate quantification of sedimentation rate was tolerable for the purposes of this study, it was essential to describe the depositional patterns accurately for future remediation studies.

Sediment deposition patterns were simulated in the main pool of Hartwell Lake using the input data representing historical records of wind and flow data. A constant temperature profile throughout the water column was specified. Effects of stratification will be discussed in the following section. A 20-day simulation of sediment transport and deposition in Hartwell Lake was conducted for the constant boundary and climate conditions specified as Case 3 in Table 1 [high inflow (465 m^3/s), high outflow (447 m^3/s), dominant southwest wind with high speed (6.8 m/s)]. At least five days of simulation were required because it takes approximately five days for sediments to settle through the 48 m water column with the specified settling velocity of 1×10^{-4} m/s, which is a typical value for fine sediments (Ziegler and Nisbet 1994). Representative conditions presented in Table 1 were used in simulations for each case since the authors were interested in the variation of sedimentation zones with respect to different wind and flow conditions.

The predicted thickness of sediment deposition in the main pool of the reservoir for two cases with distinctly different conditions, lower flows with light wind to the northeast (Case 1), and higher flows with stronger winds to the southwest (Case 3), is shown in Fig. 3. Due to the lower velocities for Case 1, more deposition was predicted to occur in this case than for Case 3. When the flow conditions in Case 3 (higher inflows and outflows) were maintained, but wind conditions corresponding to Case 1 (lower wind speeds to northeast) were used, maximum deposition rates were approximately 4% higher than for the case with higher

J. Hydraul. Eng., 2007, 133(3): 255-266

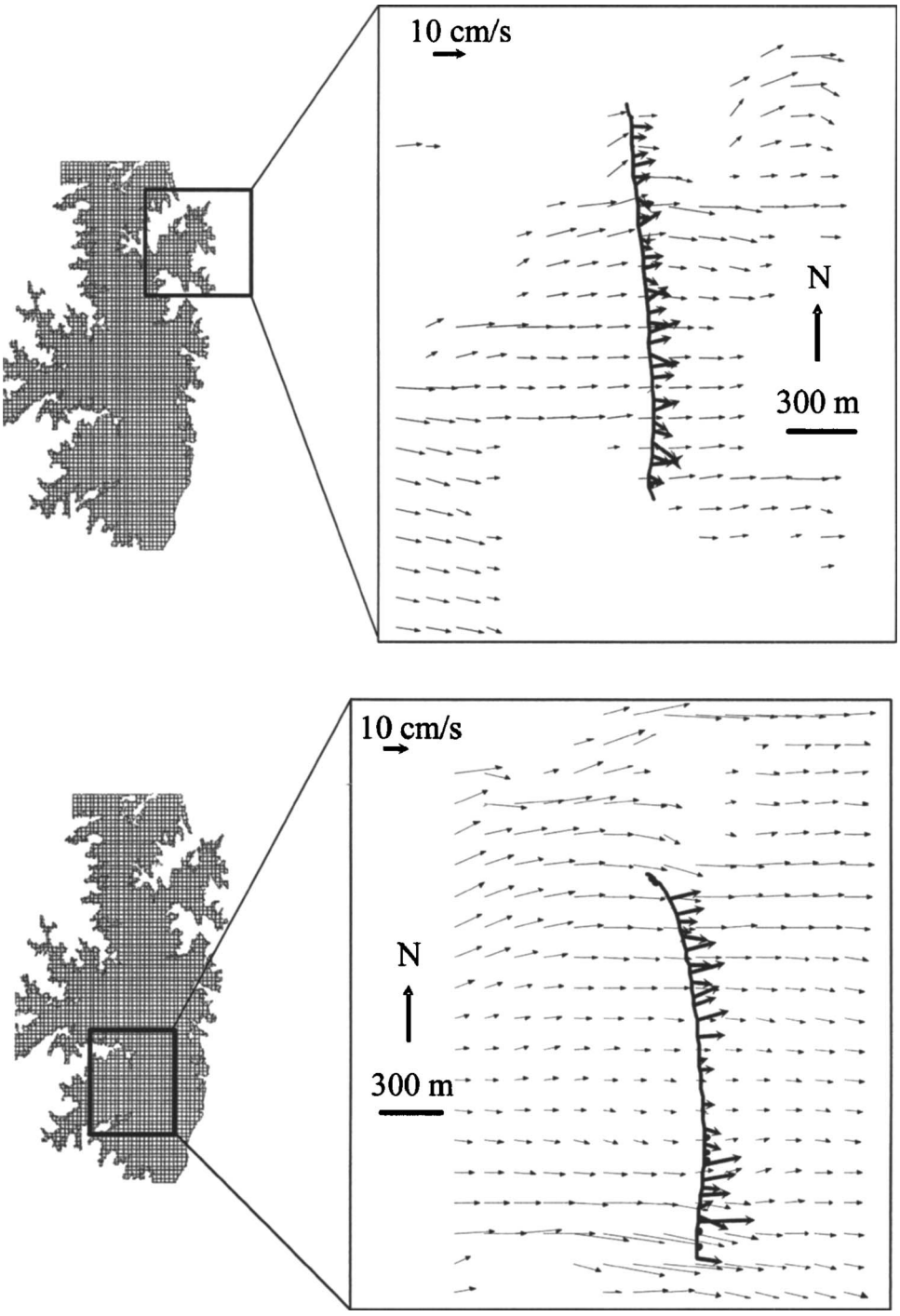

Fig. 2. Comparison of measured surface layer velocities (thick vectors, superimposed on boat track) with simulated velocities at two transects. Velocity measurements were made using an acoustic Doppler current profiler deployed from a small boat while underway. During the measurements wind was from west-southwest direction.

wind speeds, suggesting a shift in the location of depositing sediments from the thalweg to the sides of the reservoir in high wind conditions. The average deposited sediment thicknesses in the entire model domain for both cases were the same.

It was observed that deposition of sediments initially suspended in the water column dominated the deposition and lead to a uniform deposition of sediments throughout the lake. In order to reduce this effect, the initial suspended sediment concentrations were set to zero and sedimentation in the reservoir was calculated as 1 cm/year in the thalweg corresponding to the deposition of the sediments coming by the inflow. A bounding calculation approach was applied for the sediment load, in which upper (40 mg/L) and lower (10 mg/L) bounds of measured cohesive sediment concentrations corresponding to inflow were used. When this approach was applied, sedimentation patterns remained the same, although the rates did not.

Results obtained using two different equations for sediment settling velocity were compared to investigate model sensitivity. In one formulation, the settling velocity is related to the suspended sediment concentration (Ariathurai and Krone 1976). The

Table 1. Four Cases Selected for Simulation of Sediment Transport within Hartwell Lake. Wind Direction Is the Compass Heading toward Which the Wind Is Blowing

Cases	Inflow (m^3/s)	Outflow (m^3/s)	Wind speed (m/s)	Wind direction (degrees)
1. Average inflow, no outflow, dominant northeast wind with average speed	68	0	2.8	55
2. High inflow, high outflow, dominant northeast wind with high speed	465	447	6.8	55
3. High inflow, high outflow, dominant southwest wind with high speed	465	447	6.8	235
4. Moderate inflow, moderate outflow, dominant northeast wind with moderate speed	96	30	3.6	55

approach by Ziegler and Nisbet (1995), where the settling velocity is related to the median floc diameter, was used for the other formulation. Both approaches suggested that the sediments mainly deposited in the thalweg at similar rates. However, with the first formulation, more sediments were advected over greater distances and deposited closer to the dam.

Prediction of depositional flux in the EFDC model requires the specification of the critical shear stress for deposition, τ_{cd}, which depends on sediment material and floc physiochemical properties (Mehta et al. 1989). The critical stress for deposition is generally determined from laboratory or in situ measurements and values ranging from 0.06–1.1 N/m^2 have been reported in the literature. The sensitivity of model results to the critical stress for deposition was investigated. When the value of τ_{cd} was increased from 0.002 to 2 N/m^2, root-mean-square change in the sedimentation thickness calculated for the model domain was 0.5% of the maximum thickness of the deposited layer. Results were not sensitive to the specified critical deposition stress value that is usually treated as a calibration parameter in the EFDC model.

Effects of Stratification

The stability of a lake's stratification depends on many factors, most importantly the lake's depth, shape, and size. Air and water temperatures, orientation of the lake to the wind, inflow, and outflow magnitude also play roles. Lakes or reservoirs with relatively large volumes of water flowing through them (i.e., a residence time less than a month) tend not to develop persistent thermal stratification because of the mixing caused by these flows.

Fischer et al. (1979) classified the mixing regime for a strongly stratified reservoir that is under the influence of wind. They used a nondimensional ratio of the stability due to stratification com-

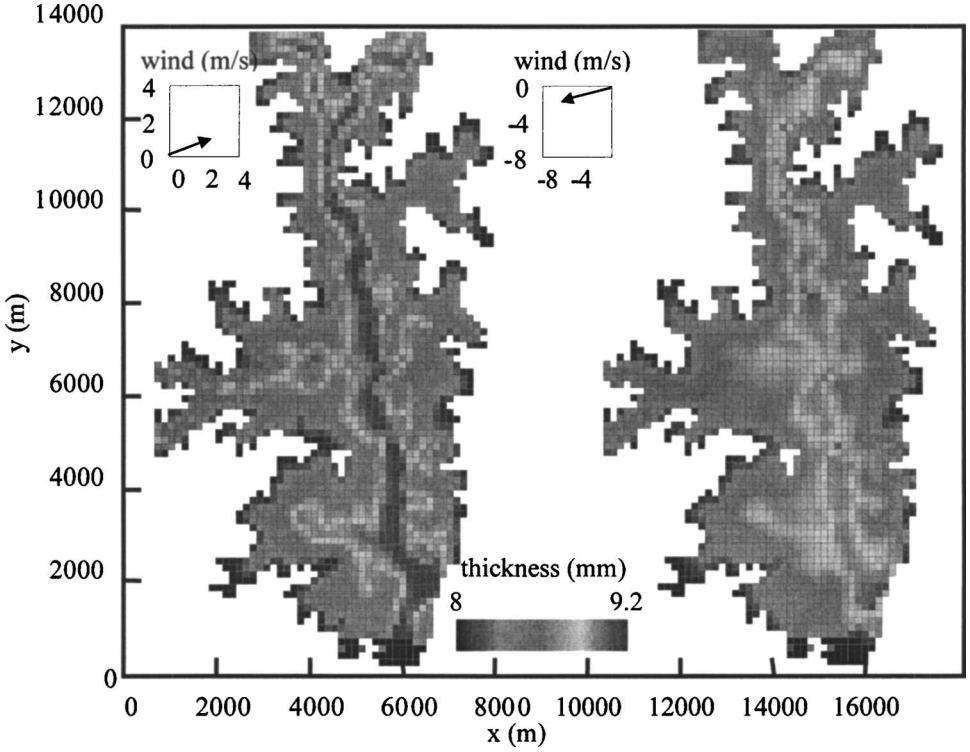

Fig. 3. Comparison of deposited sediment thickness in millimeters within Hartwell Lake after 20 days of simulation for Case 1 (left) and for Case 3 (right) in Table 1

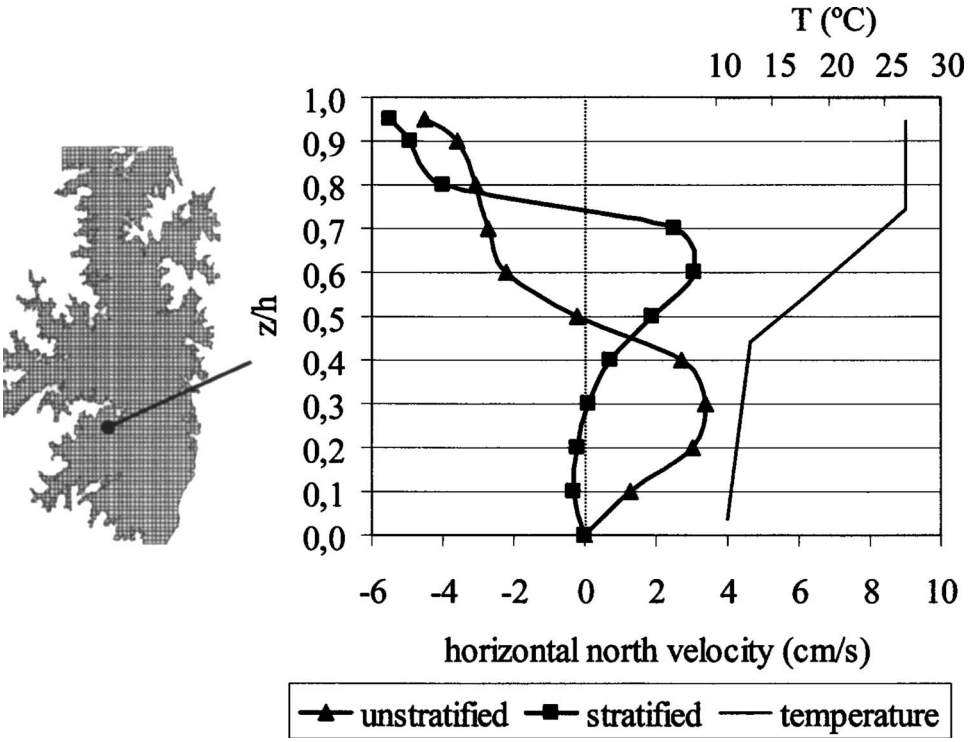

Fig. 4. Comparison of velocity profiles at a cell after five days of simulation for stratified and unstratified initial conditions. Wind is from northeast direction.

pared to the instability caused by wind-induced mixing (Richardson number)

$$\mathrm{R} = \frac{g'\bar{h}}{u_*^2} \tag{1}$$

where u_*=shear velocity due to the wind; $\bar{h}$=depth to the location of the mean density within the stratified water column; g'=reduced gravity between the epilimnion (top layer) and hypolimnion (bottom layer). The latter is defined in terms of the acceleration of gravity, hypolimnion density, ρ_h, epilimnion density, ρ_e, and average density, ρ, as

$$g' = \frac{g(\rho_h - \rho_e)}{\rho} \tag{2}$$

A typical Richardson number was calculated for Hartwell Lake for the late summer when the lake is most stratified (R=43,500 which was falling into Regime A—strongly stratified—according to Fischer's classification of mixing regimes). In Hartwell Lake, the thermocline would be expected to move vertically downward slowly as the lake is warmed.

Imberger (1998) also characterized the hydrodynamic regimes in a lake through dimensional analysis. He defined a nondimensional parameter (Lake number), L_N, in terms of the total depth of the lake, H, the height from the bottom of the lake to the seasonal thermocline, h_T, the height to the center of volume of the lake, h_V, the surface area of the lake, A_s, the shear velocity u_*, and the stability S_t, as follows:

$$L_N = \frac{S_t(H - h_T)}{u_*^2 A_s^{3/2}(H - h_V)} \tag{3}$$

where

$$S_t = \frac{1}{\rho_0}\int_0^H g(h_V - z)\rho(z)A(z)dz \cong \frac{1}{2}\left(\frac{\Delta\rho}{\rho}g\right)\frac{A_1A_2h_1h_2(h_1 + h_2)}{(A_1h_1 + A_2h_2)} \tag{4}$$

where h_1 and A_1=thickness and area of the upper layer, respectively, and h_2 and A_2=thickness and area of the bottom layer, respectively. For a typical cross section and average wind conditions in Hartwell Lake, L_N is 35, whereas for the same wind conditions, values of L_N are 20 and 12 for Mono Lake in California (MacIntyre et al. 1999) and Lake Kinneret in Israel, respectively (Imberger 1998). The critical value of L_N (L_N=1) is reached in Hartwell Lake when the wind speed is 18 m/s, whereas the critical values for the other lakes were reached for winds equal to 12 m/s (Mono) and 10 m/s (Kinneret), suggesting stronger stratification in Hartwell Lake. For winds <18 m/s and typical summer and fall stratification, there is no deep upwelling, i.e., the wind stress is insufficient to overcome buoyancy effects to upwell the water within the hypolimnion. This indicates that except for a severe storm (only 15 hourly measurements with winds >18 m/s were recorded between 1990 and 1999), the deep cold water stays within the hypolimnion during the late summer when the lake is most stratified.

Since both temperature measurements and the nondimensional parameters described above reveal strong stratification in Hartwell Lake during the late summer, the effect of stratification on deposition patterns was investigated. The typical temperature profile for September (Fig. 4) was used to define initial conditions, and thermal transport was activated in the model. Sediment deposition was modeled for the conditions given in Case 3, with the settling velocities calculated using the approach by Ziegler and Nisbet (1995).

Velocity profiles at several locations are compared for model

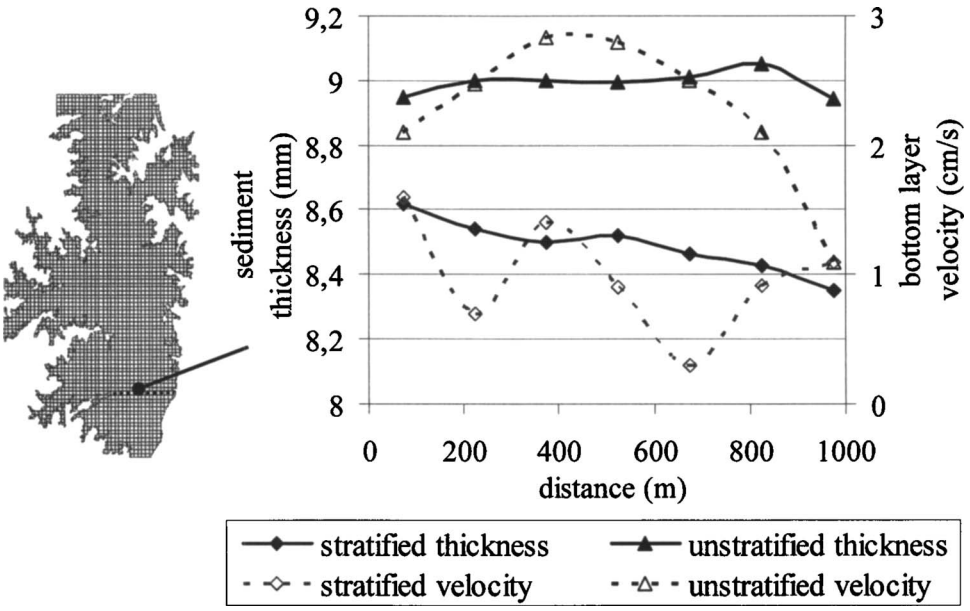

Fig. 5. Comparison of thickness of deposited layers and bottom layer velocities along a transect after 2

runs with both initially unstratified and stratified temperature profiles (Fig. 4). The depth at which the direction of flow reverses is close to mid-depth when the flow is not stratified. This point moves upward in the stratified flow case, with the flow in the direction of the wind confined to the epilimnion (warm surface layer). When the flow is stratified, the computed flow changes from a whole basin circulation to two closed gyres in the vertical plane, one in the epilimnion and the other in the hypolimnion. It was also observed that for the stratified case, the velocities near the bottom are decreased, which is thought to be due to the reduced energy transfer in the vertical direction due to the presence of the thermocline. These results were in agreement with observations made by other researchers (Rueda and Schladow 2003; Imberger 1998).

When the thickness of the deposited layer is plotted for both the stratified and unstratified initial conditions, a slight decrease (6%) in the deposition rate in the thalweg for the stratified case was observed. This decrease can be explained by the modified flow patterns due to the stratification. The stratified case features slightly larger surface velocities (Fig. 4), but once the sediment has fallen through the top third of the water column, it will not be advected further downstream, in this case. The unstratified case features a much thicker layer of water moving in the downwind direction. As a result, the unstratified case results in sediments traveling greater distances within the reservoir. This is illustrated in Fig. 5, which shows the bottom layer velocities and deposited sediment thickness along a selected transect across the thalweg.

Shoreline Erosion Quantification

A more realistic depiction of sedimentation in the reservoir requires consideration of the eroded sediments as an additional sediment source in the model. The relative importance of this source will depend on the magnitude of the erosion, and an approach that relates erosion rates to wind wave forces was developed to quantify the erosion rate of the shorelines. A simplified representation of the beach profile shape was employed. Erodibility of the cohesive shore is assumed directly proportional to the shear strength of the soil, and the erosion prediction methodology is derived based on the equation by Thorn and Parsons (1980):

$$\frac{dm}{dt} = M(\tau - \tau_c) \tag{5}$$

where m=mass of sediment eroded from the bed (kg/m^2); t=time (s); τ and τ_c=actual and critical values of the bottom shear stress (Pa); and M is an empirical coefficient relating soil resistance to erosion. This equation quantifies the erosion rate of the bed based on excess shear stress.

A schematized beach profile with uniform sediment properties, as shown in Fig. 6, was considered. Also, it was assumed that monochromatic, linear waves approach the beach. A hydropower reservoir is likely to feature deepwater waves over much of its surface area, because of the relatively small wave periods resulting from the short fetches.

Wave runup and recession rate were calculated in terms of influencing parameters such as: simplified profile shape, water level, wind direction and magnitude, and sediment characteristics.

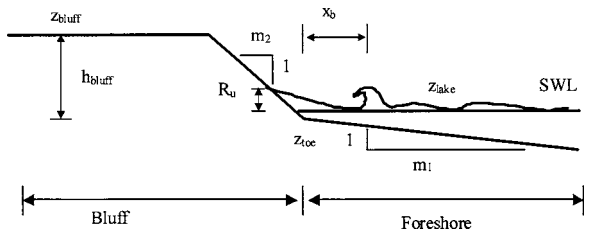

Fig. 6. Simplified geometry of shoreline, where z_{bluff} and z_{toe}=elevations of the top and toe of the bluff; z_{lake}=elevation of the lake water surface; h_{bluff}=height of the bluff measured between z_{bluff} and z_{toe}; R_u=wave runup, the local maximum or peak in the instantaneous water elevation at the shoreline; m_1 and m_2=inverse slopes of the foreshore and the bluff; x_b=distance from the toe of the bluff to the breakpoint

J. Hydraul. Eng., 2007, 133(3): 255-266

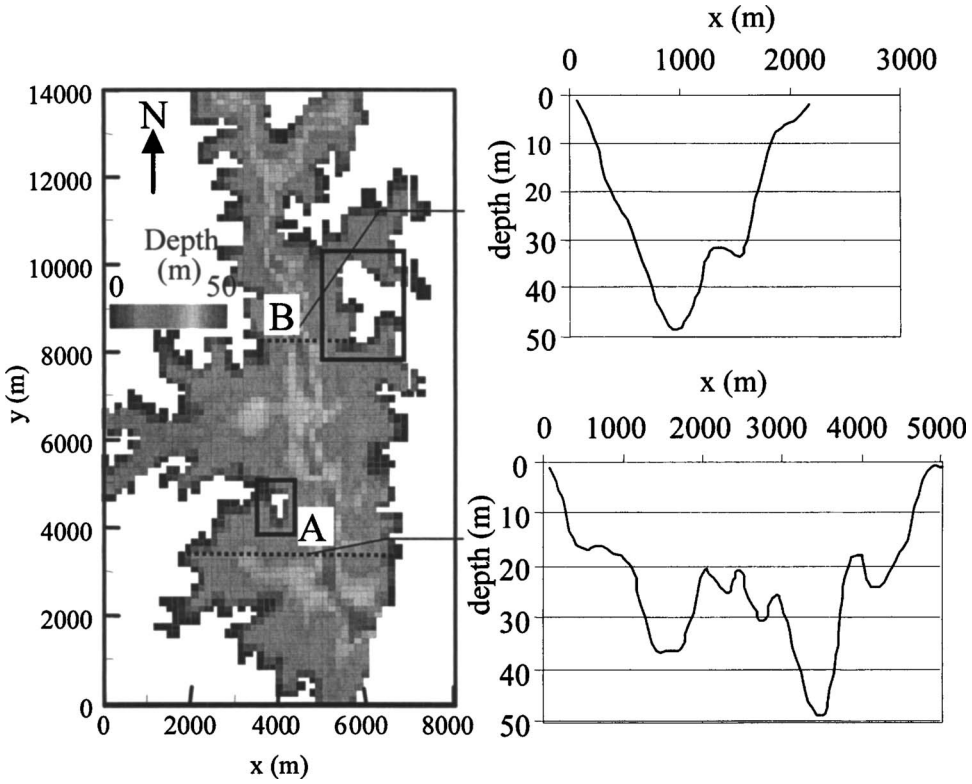

Fig. 7. Selected transects in the model domain where influences of shoreline erosion were assessed. Two peninsulas where shoreline erosion was quantified are shown by rectangles.

Recession rates are estimated for different wave runup and water level conditions. The erosion rate prediction methodology is summarized in Appendix II.

The shoreline erosion prediction methodology quantifies erosion in terms of recession rate, which is calculated as a function of instantaneous lake levels, wind direction and magnitude, fetch, and beach profile slopes. This method accounts for the variability in slopes along the shoreline of a reservoir and spatial variations in sediment characteristics. The erosion prediction methodology was applied to an eroding peninsula within the lake where the methodology was calibrated and validated using available aerial photos from different years (Elçi 2004).

After calibration based on measured changes at one location, the estimated erosion rates for other locations agreed well (errors less than 16%) with values obtained from aerial photo analysis. Average erosion rates were estimated to be about 1 m/year at the sites considered. These results were compared to those obtained by the use of other approaches (Penner 1993; Kamphius et al. 1986). Penner (1993) calculated shoreline erosion as the product of effective wave energy and an empirical material erodibility coefficient. Kamphius et al. (1986) considered two portions of the foreshore: the breaking zone, where they related erosion to wave power, and the offshore, where erosion is related to shear stresses. When these methods were applied, average erosion rates were estimated to be about 60 cm/year (40% error). The major difference between the new and existing methods is that the beach profile geometry plays a role in the new method, as it intuitively should. Following the new methodology, computed recession rates were integrated in time for the given period of interest and a final recession distance was calculated. The eroded sediment was then considered as a sediment source within the hydrodynamic model, as described in the next section.

Fate of Sediments Eroding from the Shorelines

Sediment eroded from the shoreline was treated as a source within the hydrodynamic model. It was assumed that all sediment eroded from the shoreline is put into suspension with the possibility of being advected away, providing an upper bound on the estimated influence of shoreline erosion on reservoir sedimentation.

Sediment concentrations in cells bordering the peninsulas where shoreline erosion was quantified (Fig. 7) were specified to define the strength of the sediment source. The eroding sediment concentrations were calculated by the following equation:

$$C = \frac{R \times t \times h_{\text{bluff}} \times \rho_s}{L \times d} \tag{6}$$

where R=recession rate; t=time; h_{bluff}=height of the bluff; ρ_s=sediment density; and L and d=length and depth of the computation cell, respectively. This approach assumes that all sediment eroded from the shoreline is mixed throughout the computational cell of the hydrodynamic model that borders the shoreline.

The fate of sediments eroded from the peninsulas was investigated by simulating the same wind and flow conditions with and without the contribution of sediments eroded from the shoreline. The simple case where wind was kept constant with no flows entering or exiting the model domain was considered. The deposited sediment bed thicknesses simulated with and without the contribution of the eroded sediments were compared. The sediment properties used in the simulations were the same as described previously (Appendix I).

Results revealed that sediments deposited at slightly higher

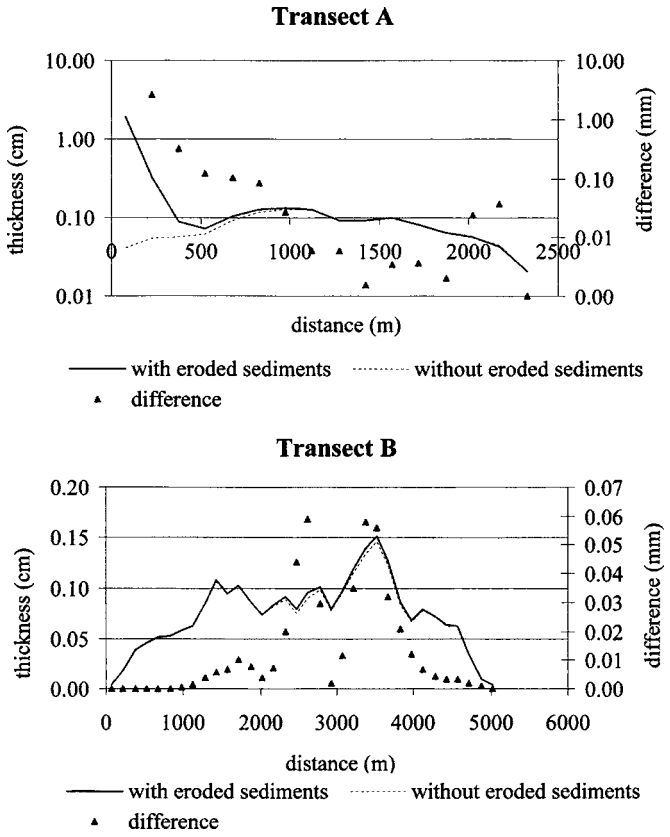

Fig. 8. The sediment deposition thicknesses at Transects A and B with and without eroding shoreline sediments after 10 days of simulation

rates in areas immediately downwind of the peninsula, compared to the case with no sediments derived from shoreline erosion. The deposition patterns in the other parts of the model domain were not affected. This is a result of the relatively small sediment influx from shoreline erosion as compared to the sediment influx from inflow, and the fact that velocities are relatively small. In fact, eroding sediments constituted 9% of the total sediments introduced to the lake.

In order to illustrate the differences in deposition patterns when the eroding sediments are introduced, two transects in the reservoir were selected (Fig. 7). The comparison of the sediment deposition thickness for these transects for the 20-day simulation is given in Fig. 8 for Transects A and B. As seen in Fig. 8, when the eroding sediments were introduced, the deposition thicknesses at the cells beside the peninsula were extremely high compared to the case where no eroded shoreline sediments were considered. This difference was reduced (2% of the thickness) along the transect further from the peninsula. When the thickness along Transect B was plotted, maximum differences were observed in the thalweg region, and were about 4% of the thickness.

Summary and Conclusions

This study involved an investigation of the hydrodynamics, sediment transport and shoreline erosion in a deep (maximum depth: 50 m), periodically strongly stratified hydropower reservoir. The primary goal was to investigate the influence of stratification and shoreline erosion on sedimentation patterns within the main pool of the reservoir. Bathymetric surveying of the lake revealed that sedimentation in the reservoir was on the order of 5 cm/year in the thalweg (2 m deposited in 40 years), where deposition was most significant. Knowledge of sedimentation patterns is essential for many different types of remediation activities, and numerical modeling can be an effective tool for predicting changes and impacts of management strategies. The study resulted in both site-specific and site-independent findings, as summarized below:

1. Sedimentation in the main pool of a reservoir was modeled using a numerical model of EFDC. The hydrodynamic results were validated using short-term velocity measurements. Depositional zones for sediment transported by the flow entering from upstream tributaries were determined using historical records of wind and flow data for the reservoir. Numerical modeling of the lake in response to different climatic forcing combinations indicated that for lower wind speeds, sediments were deposited in the thalweg of the lake regardless of the magnitudes of inflows and outflows. Higher wind speeds caused depositional zones to shift in the downwind direction.
2. The effect of stratification on velocity profiles and on sedimentation patterns was investigated. Reduced bottom layer velocities under stratified conditions resulted in less sediment reaching downstream regions of the reservoir, although total deposited volume was similar.
3. A shoreline erosion prediction methodology was developed that describes shoreline erosion as a function of lake levels, wind direction and magnitude, fetch, and beach profile shape.
4. The shoreline erosion prediction model was used to define an additional sediment source in the reservoir evolution model. Sedimentation patterns based on the sediment flux coming from tributaries and sediments eroding from shorelines were determined and the relative contribution of the eroding sediments to the overall sediment budget was discussed. It was observed that the eroding sediments had a localized impact on lake-wide deposition patterns for the study site. The proposed methodology for incorporation of the shoreline erosion process within a reservoir sedimentation model can be applied to any reservoir for more realistic prediction of sedimentation.

Further improvements to the methodology described here would include more comprehensive field measurements (inflows, local winds, suspended sediment concentrations, and temperature time series) for model calibration, validation, and better description of the model forcing. Using a network of wind stations located along the lake, rather than depending on a single station close to the lake, would improve the realism of the wind input since the effects of the topography and vegetation surrounding the reservoir would be considered. Also, in this study, sediment input to the reservoir specified at the upstream boundaries was based on a single measurement. Measurement of a suspended sediment concentration time series and the use of a rating curve obtained from these measurements would describe the sediment input to the system more precisely, and provide more accurate quantitative predictions of sedimentation rates.

Acknowledgments

This work was supported by the South Carolina Water Resources Center (SCWRC), the Georgia Water Research Institute (GWRI), and the U.S. Geological Survey (USGS).

Appendix I. EFDC Model Parameter Values Used in Sediment Transport Simulations

Model parameter	Value
SEDI: Cohesive sediment concentration (concentration) corresponding to inflow (g/m^3)	10
SEDO: Constant initial cohesive sediment concentration (g/m^3)	40
SEDBO: Constant initial cohesive sediment in bed per area (g/m^2)	1×10^4
SDEN: Sediment specific volume (m^3/g)	4×10^{-7}
SSG: Sediment specific gravity	2.65
WSEDO: Constant or reference sediment settling velocity (m/s)	1×10^{-4}
TAUD: Boundary stress below which deposition takes place (m^2/s^2)	2×10^{-3}
TAUR: Boundary stress above which surface erosion occurs (m^2/s^2)	2×10^{-3}
WRSPO: Reference surface erosion rate (g/m^2s)	0.01

Appendix II. Derivation of Shoreline Erosion Prediction Methodology

Assuming deep water conditions are valid, wind wave height, H, and period, T are predicted analytically (USACE 1998)

$$H = 4.13\times10^{-2}u_*\sqrt{\frac{X}{g}} \tag{7}$$

$$T = 2.727\times(Xu_*/g^2)^{1/3} \tag{8}$$

where X=fetch length; g=gravity, and u_*=friction velocity at the water's surface and is a function of wind speed (u) measured at 10 m elevation.

Wave runup (R_u) is written as a function of beach slope, wave height, and wave period (Battjes 1974; Hunt 1959)

$$R_u = 1.24H^{0.5}Tm_1 \tag{9}$$

For the first two cases where water level is below the toe, erodibility of the cohesive shore is assumed directly proportional to excess shear applied to the soil. Recession rate, R, is derived from a simple equation for prediction of erosion rates in the case of waves passing over a mud (Dean and Dalrymple 2001; Whitehouse et al. 2000).

The critical shear stress for erosion, τ_c (N/m^2), in terms of bed dry density T_s, as given below:

$$\tau_c = 7.95\times10^{-10}T_s^{3.64} \tag{10}$$

Assuming that the erosion rate of the bed is proportional to the excess shear stress (bed shear stress minus the critical shear stress for erosion), spatial averaging of the equation by Thorn and Parsons (1980) gives

$$\frac{dm}{dt} = M_2(\overline{\tau-\tau_c}) \tag{11}$$

The mean value of the bed shear stress within the surf zone, wherever this bed shear stress exceeds the critical value can be calculated as

$$\overline{\tau-\tau_c} = \frac{1}{x}\int_0^x(\tau-\tau_c)dx = \frac{1}{x}\int_0^x\left(\frac{1}{8}\rho f_w\frac{\pi^2H^2}{T^2\sinh^2(kh)}-\tau_c\right)dx \tag{12}$$

Recession rate, R (m/s) is assumed proportional to the erosion rate, dm/dt ($kg/m^2/s$). The upper limit in Eq. (12) is replaced by x_b, which is the distance to the breakpoint. The depth used in the calculations is the depth at breaking. Dividing the erosion rate by sediment density, ρ_s (kg/m^3), recession rate, R (m/s), is then obtained, where an empirical factor describing the eroding effect of wave runup on the bluff, n(=3), wetness ratio, λ (varying between 0 and 1) and κ(=0.78)

$$R = \frac{M_2}{\rho_s}\left(\frac{1}{6}\rho f_w\kappa^2\pi^2m_1^2\frac{x_b^2}{T^2\sinh^2(kh)}-\tau_c\right)(1+n\lambda) \tag{13}$$

For the last case where water level is above the toe of the bluff, the erodibility of the cohesive soil is related to wave power, which can be calculated as a function of wave height. For this case, the recession is derived from the equation for volume transport rate (USACE 1998)

$$Q = KH_b^{5/2} \tag{14}$$

where K=parameter function of the wave height, wave period and slope (Kamphuis and Readshaw 1966)

$$Q = f(H^2,T,m_1) \tag{15}$$

Dividing the equation for volume transport rate by unit area, multiplying by the wetness ratio λ, and the calibration coefficient, C, the equation for recession rate is derived

$$R = C\lambda H^2Tm_1 \tag{16}$$

For slopes steeper than 1:15, Eq. (16) is modified to account for the bluff slope m_2 (Newe et al. 1999)

$$R = C\lambda H^2Tm_1m_2 \tag{17}$$

The following list summarizes the steps for application of the erosion rate prediction methodology:

1. Wind speed, wind direction, and water level data are obtained. Fetches are measured on a map for each location and wind direction.
2. Geometry of the shoreline of interest is surveyed or estimated from a topographic map and values of z_{bluff}, z_{toe}, z_{lake}, h_{bluff}, m_1, and m_2 are measured or estimated.
3. Wave runup (R_u) is calculated and is added to the water level and compared with the elevation of the toe of the bluff:
   - If the water level + wave runup is below the toe ($z_{lake}+R_u<z_{toe}$), recession rate is assumed proportional to the erodibility of the cohesive shore. Erodibility is calculated in terms of excess shear applied to the soil [Eq. (13)].
   - If the water level is below the toe ($z_{lake}<z_{toe}$) but the water level + wave runup is above the toe ($z_{lake}+R_u>z_{toe}$), then the recession rate R (m/s) is calculated using Eq. (13) where λ is nonzero.
   - If the water level is above the toe ($z_{lake}>z_{toe}$), then erodibility of the cohesive soil is related to wave power that can be calculated as a function of wave height [Eq. (17)].
4. Recession rates (in meters/h) are integrated in time for the given period of interest and a final recession distance is calculated.

Notation

The following symbols are used in this paper:

A_s = surface area of the lake;
d = depth of computational cell;
g = gravity;
g' = reduced gravity;
H = wave height;
H_L = total depth of the lake;
h_{bluff} = bluff height;
h_T = height from the bottom of the lake to the seasonal thermocline;
h_V = height to the center of volume of the lake;
L = length of computational cell;
L_N = dimensionless Lake number;
M = empirical sediment erodibility coefficient;
m = mass of sediment eroded from the bed per unit area;
m_1 = beach slope;
m_2 = bluff slope;
Q = volume transport rate;
R = recession rate;
R_u = wave runup;
S_t = stability;
t = time;
T = wave period;
T_s = bed dry density;
u = wind speed;
u_* = friction velocity;
X = fetch length;
x_b = distance to the break point;
z_{bluff} = elevation of the bluff;
z_{lake} = elevation of the lake;
z_{toe} = elevation of the toe;
ρ = average density;
ρ_e = epilimnion density;
ρ_h = hypolimnion density;
ρ_s = sediment density; and
τ_c = critical shear stress for erosion.

References

Ariathurai, R., and Krone, R. B. (1976). "Finite element model for cohesive sediment transport." *J. Hydr. Div.*, 102(3), 323–338.

Battjes, J. A. (1974). "Computation of setup, longshore currents, runup, and overtopping due to wind generated waves." *Rep. No. 74-2*, Civil Engineering Dept., Delft Univ. of Techology, Dalft, The Netherlands.

Blumberg, A. F., and Mellor, G. L. (1987). "A description of a three-dimensional coastal ocean circulation model." *Three-dimensional coastal ocean models*, N. S. Heaps, ed., American Geophysical Union, Washington, D.C., 1–16.

Blumberg, A. F., Khan, L. A., and St. John, J. P. (1999). "Three-dimensional hydrodynamic model of New York Harbor Region." *J. Hydraul. Eng.*, 125(8), 799–815.

Clearwater. (1997). "PCB contamination of the Hudson." ⟨http://www.clearwater.org/news/hazard.html⟩ (April 7, 1997).

Dean, R. G., and Dalrymple, R. A. (2001). *Water wave mechanics for engineers and scientists*. World Scientific, Singapore.

Elçi, S. (2004). "Modeling of hydrodynamic circulation and cohesive sediment transport and prediction of shoreline erosion in Hartwell Lake, SC/GA." Ph.D. thesis, Georgia Institute of Technology.

Falconer, R. A., George, D. G., and Hall, P. (1991). "Three-dimensional numerical modeling of wind driven circulation in a shallow homogeneous lake." *J. Hydrol.*, 124(1), 59–79.

Fischer, H. B., List, E. G., Koh, R. C.Y., Imberger, J., and Brooks, N. H. (1979). *Mixing in inland and coastal waters*, Academic, New York.

Hamrick, J. M. (1996). "User's manual for the environmental fluid dynamics computer code." *Special Rep. No. 331*, The College of William and Mary, Gloucester Point, Va.

Hunt, I. A. (1959). "Design of seawalls and breakwaters." *Control Eng. Pract.*, 85(3), 123–152.

Imberger, J. (1998). *Physical processes in lakes and oceans*, AGU Coastal and Estuarine Studies, Vol. 54, AGU, Code CE0542685.

Ji, Z.-G., Morton, M. R., and Hamrick, J. M. (2000). "Modeling hydrodynamic and sediment processes in Morro Bay." *Estuarine and Coastal Modeling: Proc., 6th Int. Conf.*, M. L. Spaulding and H. L. Butler, eds., ASCE, New York, 1035–1054.

Ji, Z.-G., Morton, M. R., and Hamrick, J. M. (2001). "Wetting and drying simulation of estuarine processes." *Estuarine Coastal Shelf Sci.*, 53, 683–700.

Jin, K.-R., Hamrick, J. H., and Tisdale, T. (2000). "Application of a three-dimensional hydrodynamic model for Lake Okeechobee." *J. Hydraul. Eng.*, 126(10), 758–771.

Jin, K. R., and Ji, Z.-G. (2001). "Calibration and verification of a spectral wind-wave model for Lake Okeechobee." *Ocean Eng.*, 28(5), 571–584.

Jin, K. R., Ji, Z.-G., and Hamrick, J. M. (2002). "Modeling winter circulation in Lake Okeechobee, Florida." *J. Waterway, Port, Coastal, Ocean Eng.*, 128(3), 114–125.

Kamphuis, J. W., Davies, M. H., Nairn, R. B., and Sayao, O. J. (1986). "Calculation of littoral sand transport rate." *Coastal Eng.* 10(1), 1–21.

Kamphuis, J. W., and Readshaw, J. S. (1979). "Model study of alongshore sediment transport rate." *Proc., 16th Coastal Eng. Conf.*, Vol. 2, 1656–1674.

Kim, S. C., Wright, L. D., and Kim, B. O. (1997). "The combined effects of synoptic-scale and local-scale meteorological events on bed stress and sediment transport on the inner shelf of the Middle Atlantic Bight." *Cont. Shelf Res.*, 17(4), 407–433.

MacIntyre, S., Flynn, K. M., Jellison, R., and Romero, J. R. (1999). "Boundary mixing and nutrient fluxes in Mono Lake, California." *Soc. Pet. Eng. J.*, 44(3), 512–529.

Mehta, A. J., et al. (1989). "Cohesive sediment transport. Part 1: Process description. Part 2: Application." *J. Hydraul. Eng.*, 115(8), ASCE, 1076–1112.

Nairn, R. B., Pinchin, B. M., and Philpott, K. L. (1986). "A cohesive coast development model." *Proc., Symp. on Cohesive Shores*, National Research Council Canada, Associate Committee on Shorelines, 246–261.

Newe, J., Peters, K., and Dette, H. H. (1999). "Profile development under storm conditions as a function of beach slope." *Proc., 4th Int. Symp. On Coastal Eng.*, ASCE, Reston, Va., 2582–2596.

Penner, L. A. (1993). "Shore erosion and slumping on Western Canadian lakes and reservoirs—A methodology for estimating future bank erosion rates." Environment Canada, Regina, Sask.

Rueda, F. J., and Schladow, S. G. (2003). "Dynamics of a large polymictic lake. II: Numerical simulations." *J. Hydraul. Eng.*, 129(2), 92–101.

Shen, J., Boon, J. D., and Kuo, A. Y. (1999). "A modeling study of a tidal intrusion front and its impact on larval dispersion in the James River estuary, Virginia." *Estuaries*, 22(3a), 681–692.

Shen, J., and Kuo, A. Y. (1999). "Numerical investigation of an estuarine front and its associated eddy." *J. Waterway, Port, Coastal, Ocean Eng.*, 125(3), 127–135.

TetraTech (1999). "Theoretical and computational aspects of sediment transport in the EFDC model." *Technical Rep. Prepared for U.S. Environmental Protection Agency*, Tetra Tech, Inc., Fairfax, Va.

Thorn, M. F.C., and Parsons, J. G. (1980). "Erosion of cohesive sediments in estuaries: An engineering guide." *Proc., Int. Symp. on Dredging Technol.*, 349–358.

U.S. Army Corps of Engineers (USACE). (1998). *Coastal engineering manual, part III*, Dept. of the Army, Washington, D.C.

U.S. Environmental Protection Agency (USEPA). (1991). "Sangamo-Weston Inc./Twelve-Mile Creek/Lake Hartwell PCB contamination." ⟨http://www.epa.gov/oerrpage/superfund/sites/npl/nar486.htm⟩.

Whitehouse, R., Soulsby, R., Roberts, W., and Mitchener, H. (2000). *Dynamics of estuarine muds*, Thomas Telford, London.

Yang, Z., Khangaonkar, T., DeGasperi, C., and Marshall, K. (2000). "Three-dimensional modeling of temperature stratification and density-driven circulation in Lake Billy Chinook, Oregon." *Proc., 6th Int. Conf. Estuarine and Coastal Modeling*, ASCE, Reston, Va., 411–425.

Ziegler, C. K., and Nisbet, B. (1994). "Fine-grained sediment transport in Pawtuxet River, Rhode Island." *J. Hydraul. Eng.*, 120 (5), 561–576.

Ziegler, C. K., and Nisbet, B. (1995). "Long-term simulation of fine-grained sediment transport in large reservoir." *J. Hydraul. Eng.*, 121 (11), 773–781.